Letter

Quantum viscosity and the Reynolds similitude of a pure superfluid

Hiromitsu Takeuchi [*]
Department of Physics and Nambu Yoichiro Institute of Theoretical and Experimental Physics (NITEP), Osaka Metropolitan University, 3-3-138 Sugimoto, Sumiyoshi-ku, Osaka 558-8585, Japan

(Received 21 February 2023; revised 15 June 2023; accepted 21 November 2023; published 11 January 2024)

The Reynolds similitude, a key concept in hydrodynamics, states that two phenomena of different length scales with a similar geometry are physically identical. Flow properties are universally determined in a unified way in terms of the Reynolds number $\mathcal{R}$ (dimensionless, ratio of inertial to viscous forces in incompressible fluids). For example, the drag coefficient c_D of objects with similar shapes moving in fluids is expressed by a universal function of $\mathcal{R}$. Certain studies introduced similar dimensionless numbers, that is, the superfluid Reynolds number $\mathcal{R}_s$, to characterize turbulent flows in superfluids. However, the applicability of the similitude to inviscid quantum fluids is nontrivial as the original theory is applicable to viscous fluids. This Letter proposes a method to verify the similitude using current experimental techniques in quantum liquid He II. A highly precise relation between c_D and $\mathcal{R}_s$ was obtained in terms of the terminal speed of a macroscopic body falling in He II at finite temperatures across the Knudsen (ballistic) and hydrodynamic regimes of thermal excitations. The Reynolds similitude in superfluids proves the quantum viscosity of a pure superfluid and can facilitate a unified mutual development of classical and quantum hydrodynamics; the concept of quantum viscosity provides a practical correspondence between classical and quantum turbulence as a dissipative phenomenon.

DOI: 10.1103/PhysRevB.109.L020502

The Reynolds number $\mathcal{R}$ is a dimensionless parameter that characterizes fluid flows on different length scales in a unified manner [1]. It is the ratio of inertial to viscous forces in the Navier-Stokes equation $\mathcal{R} = \frac{ud}{\nu}$, where ν is the kinematic viscosity, and u and d are the characteristic speed and length, respectively. The Reynolds law of dynamic similarity or Reynolds similitude states that two fluid flows around similar structures with different length scales are hydrodynamically identical provided they exhibit the same $\mathcal{R}$ value [2]. Considering the drag force on a body moving in a fluid, the drag coefficient c_D is universally described as a function of $\mathcal{R}$ from a laminar flow with low $\mathcal{R}$ to a high-$\mathcal{R}$ flow with turbulent wake. The similitude provides a universal view of flow phenomena in nature and is applicable to flows at any length scales such as global air movement and blood circulation in the body. However, it is yet to be applied to superfluids. The Reynolds number is ill defined in superfluids owing to the lack of viscosity due to the quantum effect, called superfluidity [3].

Consequently, the concept of a *superfluid Reynolds number* has garnered attention in the fields of quantum gases and liquids. Nore and collaborators introduced this concept in their earlier works on superfluid turbulence in the Gross-Pitaevskii model [4,5]. They observed an energy spectrum compatible with the Kolmogorov law in the inertial range where fluid viscosity does not affect turbulent eddies on length scales larger than the Taylor microscale $\sim\frac{d}{\sqrt{\mathcal{R}}}$ [6]. The superfluid Reynolds number $\mathcal{R}_s$ is then defined by its quantum counterpart $\lambda = \frac{d}{\sqrt{\mathcal{R}_s}}$. Neglecting the difference in number factors, it is defined as

$$\mathcal{R}_s = \frac{ud}{\nu_s}, \tag{1}$$

where the *quantum* kinematic viscosity ν_s is in the order of h/m with Planck constant h and mass m of the constituent particles of the superfluid. The quantum viscosity implies effective dissipation on length scales smaller than λ at absolute zero, while normal viscosity due to thermal excitations can occur only at finite temperatures. Subsequently, Eq. (1) is applied to different superfluids accompanied with the physical identification of ν_s using the circulation quantum κ of the quantum vortex considering that a collection of quantum vortices mimics a classical vortex with continuous vorticity; superfluid turbulence on the length scale considerably exceeding the mean distance between quantum vortices obeys the Kolmogorov law of *classical* turbulence [7]. Although such a continuum approximation of vortices is considered intuitively reasonable and the Kolmogorov spectrum has been realized [8] in the dissipationless inertial range, the validity of Eq. (1) is quite nontrivial owing to the lack of experimental justification. Recently, Reeves *et al.* proposed a correction of $\mathcal{R}_s$, wherein u in Eq. (1) was replaced as $u \to u - u_c$ incorporating the critical velocity u_c for vortex generation [9]. Despite the qualitative consistency of these predictions with experiments [10–13], a dynamic similarity has not been established because of the u_c dependence on the system details. Thus, a universal description of complicated flows interacting with moving bodies in superfluids remains elusive, in contrast to the considerable research on the Reynolds similitude in classical hydrodynamics.

Therefore, we theoretically propose a protocol for verifying the Reynolds similitude in superfluid He II. The similitude

[*]takeuchi@omu.ac.jp; http://hiromitsu-takeuchi.appspot.com

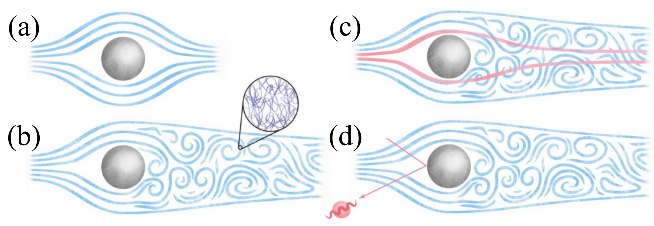

FIG. 1. Schematics of the wake behind a sphere moving from the right to left in quantum liquid He II. (a) Drag is zero without quantum vortices at $T = 0$. (b) Coarse-grained quantum vortices reproduce a turbulent wake with high $\mathcal{R}(= \mathcal{R}_s)$ according to the Reynolds similitude extended to superfluids. The inset represents a microscopic view of quantum vortices in the turbulent wake. (c) At finite temperatures in the hydrodynamic regime ($l_{\rm MFP} \ll d$), quasiparticles form a Stokes flow in the presence of a turbulent wake in the superfluid component. (d) Quasiparticles form a dilute gas and the drag is caused by their ballistic scattering in the Knudsen regime ($l_{\rm MFP} \gg d$).

could be examined through a terminal speed measurement of a body falling in the superfluid at finite temperatures. The combined analyses of classical and quantum hydrodynamics confirm a relation between the drag coefficient c_D and $\mathcal{R}_s$ in terms of the terminal speed by considering the thermal correction below 1.5 K. The proposed theory is also consistent with the observation of a complicated motion of ^{4}He crystals falling in He II [14], which is caused by a turbulent wake in the superfluid with high $\mathcal{R}_s$. Establishing the similitude in superfluids is an essential step to unify classical and quantum hydrodynamics.

Drag coefficients. Consider a rigid body of size d falling with a constant speed u in He II at finite temperatures. This situation is realized when the drag force F_D on the body by a quantum liquid balances the net force $F_G = (\gamma - 1)\rho V_R g$ of gravity and buoyancy. Here, ρ is the fluid density, g the gravitational acceleration, $M_R = \gamma\rho V_R$ the body mass with volume $V_R \sim d^3$, and $\gamma = M_R/(V_R\rho)$ the mass density ratio of the body and liquid. He II comprises two independent fluid components: a normal fluid and superfluid components in a two-fluid model [3]. The former is a conventional fluid with viscosity, comprising thermal excitations (quasiparticles) such as phonons and rotons. The latter behaves as an ideal inviscid fluid. Accordingly, F_D is divided into two contributions, F_n and F_s, from the normal fluid and superfluid components, respectively; $F_D = F_n + F_s$. The kinematic viscosity ν_n of the normal fluid component has been well studied [15–29] and the normal Reynolds number is $\mathcal{R}_n = \frac{ud}{\nu_n}$.

At zero temperature ($T = 0$), only the superfluid component exists with the body never experiencing the drag force $F_D = 0$, which is known as the D'Alembert's paradox [2] [Fig. 1(a)]. This is not true when quantum vortices appear leading to the *quantum* viscosity ν_s. The forces are formulated as

$$F_{n,s} = \tfrac{1}{2} c_{n,s}\rho_{n,s} S_R u^2, \tag{2}$$

with the normal fluid density ρ_n, the superfluid density $\rho_s = \rho - \rho_n$, and the project area $S_R \sim d^2$ of the body. To perform quantitative analyses, an empirical form of the drag coefficient $c_n \equiv c_D(\mathcal{R}_n)$ [30–32] was applied,

$$c_D(\mathcal{R}) = \frac{24}{\mathcal{R}} c_1 + \frac{4}{\sqrt{\mathcal{R}}} c_2 + c_3, \tag{3}$$

with $c_{1,2,3} = O(1)$ up to $\mathcal{R}_n \sim 10^5$, e.g., $(c_1, c_2, c_3) = (1, 1, 0.4)$ for spheres. The applicability of this law to c_s is nontrivial as the quantum viscosity ν_s is a hypothetical concept here [Fig. 1(b)]. Hereafter, we assume $\nu_s = \kappa = h/m$ with the atomic mass m of ^{4}He.

Thus, this Letter proposes a method to test the validity of $c_s = c_D(\mathcal{R}_s)$. The relation between c_s and $\mathcal{R}_s$ can be investigated by observing the terminal speed of the body with certain corrections. At finite temperatures, the normal fluid component causes a thermal correction. Even at zero temperature, certain nonthermal corrections can occur in Eq. (1), $u \to u + \delta u$ and $d \to d + \delta d$, which hinder the extraction of the universal behavior of the dynamic similarity because the corrections are dependent on extrinsic factors related to the details of the systems.

The velocity and size corrections, δu and δd, are related to various mechanisms associated with the vortex generation and the micro- and mesoscopic structures on the body surface [33]. The roughness of the surface can facilitate the size correction primarily. According to Ref. [34], quantum vortices form a boundary layer at a distance $l_{\rm rough}$, the height of the highest "mountain" on the rough surface of a material, resulting in $\delta d = l_{\rm rough} \sim 10^{-6}$ m. As the drag force works only when quantum vortices exist, the velocity correction may be in the order of the vortex-generation velocity u_c, $\delta u \sim -u_c$, as proposed in Ref. [9]. The criterion u_c can be much smaller than u for a macroscopic body in He II. The smallest value of $u_c \sim 0.001$ m/s has been reported for large-scale objects [35,36]. Inherently, the turbulence transition by vortex generation is an event of the first-order phase transition involving hysteresis and thus the critical velocity varies depending on fluctuations [37–40]. Such a variation does not affect the drag in the final turbulent state, suggesting that u_c could be irrelevant to the drag provided turbulent wakes are realized for $u \gg u_c$. Regardless, these corrections may be negligible in our system when $\delta d/d \ll 1$ and $|\delta u|/u \ll 1$, in contrast to the systems of atomic quantum gases [11,12], where the corrections cannot be neglected.

Terminal speed. By neglecting the above nonthermal corrections, the terminal speed is derived from $F_D = F_G$ as

$$u = (1 - \delta_{\rm th})\bar{u}_T, \tag{4}$$

with the thermal correction

$$\delta_{\rm th} = 1 - \sqrt{\frac{1 + \rho_n/\rho_s}{1 + F_n/F_s}}, \tag{5}$$

and the terminal speed without any correction

$$\bar{u}_T = \sqrt{\frac{2g(\gamma - 1)}{c_D(\mathcal{R}_s)}\frac{V_R}{S_R}}. \tag{6}$$

For reference, the relation of $\mathcal{R}_s$ to d and $\bar{u}_T$ is shown in Fig. 2, where we used $V_R/S_R = 2d/3$ and $d(\mathcal{R}_s) = [\frac{3\kappa^2 c_s \mathcal{R}_s^2}{4g(\gamma-1)}]^{1/3}$ for spheres. An iron ball ($\gamma = 45.8$) of diameter $d = 0.9$ mm

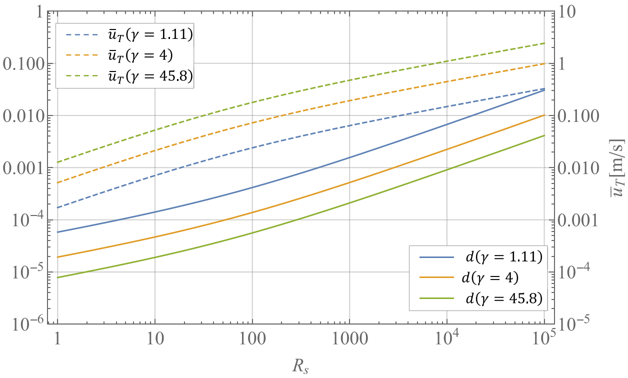

FIG. 2. Plots of the relation of $\mathcal{R}_s$ to the diameter d (solid) and the terminal speed $\bar{u}_T$ (dashed) for spheres in He II under vapor pressure at $T = 0$ K. Blue, yellow, and green curves correspond to the results for $\gamma = 1.11$ (^{4}He crystal), $\gamma = 4$, and $\gamma = 45.8$ (iron), respectively.

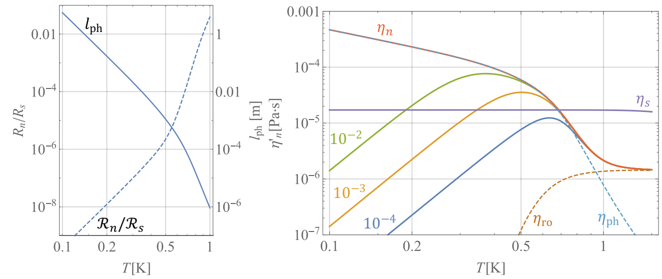

FIG. 3. Temperature dependence of (left) $\mathcal{R}_n/\mathcal{R}_s$, $l_{\rm ph}$, and (right) η'_n with $C = 3/5$ for spheres of radius $d = 10^{-4}$, 10^{-3}, and 10^{-2} m. For reference, we also plot $\eta_{n,{\rm ph},{\rm ro},s}$ and η'_n. We have $\eta'_n \propto T^4$ in the Knudsen limit ($l_{\rm ph} \gg d$).

can realize $\mathcal{R}_s \sim 10^4$ with $u_T = 1.1$ m/s, thus satisfying our requirements of $\delta d/d \ll 1$ and $\delta u/u \ll 1$ to neglecting the nonthermal corrections. These estimations do not change essentially provided regularly shaped bodies with $V_R/S_R \sim d$ are considered.

Moreover, the above estimation explains the observation [14] quantitatively, yielding a result of $u_T \approx 0.06$ m/s and $\mathcal{R}_s = 10^3$ for a ^{4}He crystal with $d \approx 1.56$ mm and $\gamma = 1.11$ [41]. Thus, the chaotic property of the turbulent wake with many vortices for $\mathcal{R}_s = 10^3$ results in the complicated motion of the falling ^{4}He crystal. This consistency suggests that the Reynolds similitude is applicable to quantum liquid He II even when neglecting the thermal correction.

Thermal correction. To systematically examine the Reynolds similitudes including the thermal correction, we formulate the reduced quantities of $\mathcal{R}_s$ and c_D in terms of the observables u and $\delta_{\rm th}$ as follows,

$$\bar{\mathcal{R}}_s = \frac{\mathcal{R}_s}{1 - \delta_{\rm th}} = \frac{ud}{(1 - \delta_{\rm th})\kappa}, \tag{7}$$

$$\bar{c}_s = \frac{2g(\gamma - 1)}{u^2} \frac{V_R}{S_R} (1 - \delta_{\rm th})^2. \tag{8}$$

These are the fundamental equations of this Letter; the similitude is established if the plot of $(\bar{\mathcal{R}}_s, \bar{c}_s)$ coincides with the hypothetical relation of $\bar{c}_s = c_D(\bar{\mathcal{R}}_s)$. The thermal correction $\delta_{\rm th}$ must vanish without thermal excitations and is small compared with unity in a wide range of experimental parameters as shown later, which is determined by the factors $\frac{\rho_n}{\rho_s}$ and $\frac{F_n}{F_s}$. The temperature dependence of $\frac{\rho_n}{\rho_s} = \frac{\rho_n}{\rho - \rho_n}$ is well known both experimentally and theoretically and can be computed precisely by regarding the normal fluid component as a sum of the thermal distributions of phonons and rotons ($\rho_n = \rho_{\rm ph} + \rho_{\rm ro}$) [3]. The main task is to compute $\frac{F_n}{F_s}$, which is determined by T and $\mathcal{R}_s$.

To solve the problem step by step, first, we evaluate the ratio

$$\frac{\mathcal{R}_n}{\mathcal{R}_s} = \frac{\nu_s}{\nu_n} = \frac{\eta_s}{\eta_n} \frac{\rho_n}{\rho_s}, \tag{9}$$

with the normal dynamic viscosity $\eta_n = \rho_n \nu_n$ and $\eta_s \equiv \rho_s \kappa$. Within our restriction of $\mathcal{R}_s \lesssim 10^5$ we have $\mathcal{R}_n \lesssim 1$ with $\mathcal{R}_n/\mathcal{R}_s \lesssim 10^{-4}$ for $T \lesssim 0.7$ K [Fig. 3 (left)]. Subsequently, the normal fluid component is considered as laminar and the Stokes-type law $F_n = F_H \equiv 12 c_1 \eta_n S_R u/d$ is applied with $c_D(\mathcal{R}_n) \approx \frac{24}{\mathcal{R}_n} c_1$ below 0.7 K [Fig. 1(c)].

A misassumption may be that the thermal correction is negligible as the effect of the normal fluid component is typically neglected compared with the superfluid component under such low temperatures (e.g., $\rho_n/\rho_s \ll 0.1$ for $T < 1$ K [33]). However, η_n is known to diverge to infinity for $T \to 0$ and thus F_n can increase rapidly with decreasing T. This unphysical divergence is owing to the breakdown of the hydrodynamic description for the normal fluid component in the Knudsen regime ($\mathcal{K} \equiv l_{\rm MFP}/d \gg 1$) with the mean free path (MFP) $l_{\rm MFP}$ of quasiparticles. As measured for oscillating objects [42,43], the normal drag force actually decreases with T in the Knudsen regime because quasiparticles are dilute and they rarely collide with the body at lower temperatures [Fig. 1(d)]. These contrasting temperature dependences between two regimes render the quantitative description of the thermal correction from the Knudsen regime to the hydrodynamic one ($\mathcal{K} \ll 1$) challenging.

To formulate the Knudsen-hydrodynamic crossover of F_n, we propose an empirical method, which has succeeded quantitatively in a similar problem regarding the drag force on a porous media immersed in Landau-Fermi liquid ^{3}He [44,45]. The method for fermionic quasiparticles was extended to our system of bosonic quasiparticles. The crossover is characterized by the Knudsen number $\mathcal{K}$, and η_n is replaced by

$$\eta'_n = \frac{1}{1 + C\mathcal{K}} \eta_n, \tag{10}$$

where C is the Cunningham constant. The normal drag force is expressed as

$$F_n = 12 c_1 \eta'_n S_R u/d, \tag{11}$$

which reduces F_H in the hydrodynamic limit $\mathcal{K} \to 0$. If the analysis is confined to a macroscopic body of $d \gtrsim 10^{-4}$ m, the crossover ($\mathcal{K} \sim 1$) occurs below $T \lesssim 0.7$ K, where $l_{\rm MFP}$ is well described by the lifetime $\tau_{\rm ph}$ of phonons as $l_{\rm ph} = u_{\rm ph} \tau_{\rm ph}$ with the phonon velocity $u_{\rm ph} = 238$ m/s [Fig. 3 (left)]. Subsequently, $C = \frac{12 c_1}{5} \frac{S_R}{\sigma_{\rm tr}}$ because of the constraint that, for

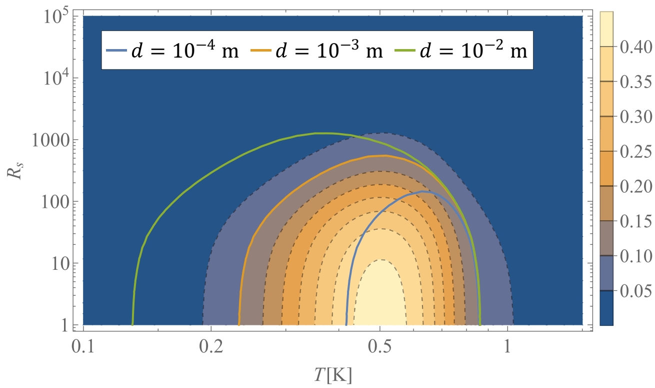

FIG. 4. Plot of thermal correction $\delta_{\rm th}$ for $d = 10^{-3}$ m. The solid curves shows the contour of $\delta_{\rm th} = 0.1$ for $d = 10^{-4}$, 10^{-3}, and 10^{-2} m.

$\mathcal{K} \to \infty$, F_n coincides with $F_K \equiv u_{\rm ph}\rho_n\sigma_{\rm tr}u$, where $\sigma_{\rm tr}(\sim d^2)$ is the transport cross section in the kinetic theory of quasiparticle gases.

Here, Eq. (10) is quantitatively validated via plots of η'_n in Fig. 3 (right) with a fixed value of $\sigma_{\rm tr}/S_R = 4$ ($C = 3/5$). They were consistent with the existing observations of the "effective" viscosity associated with the drag force [29]. An estimation of η_n was adopted from the preceding studies [15–29], which is divided into the contributions from phonons and rotons, $\eta_n = \eta_{\rm ph} + \eta_{\rm ro}$ [33]. While the roton part $\eta_{\rm ro}$ is dominant and independent on T for $1 < T \lesssim 1.5$ K, the phonon part $\eta_{\rm ph}$ is important below 0.7 K and increases with decreasing temperature, $\eta_{\rm ph} = \frac{1}{5}\rho_n u_{\rm ph}^2\tau_{\rm ph}$ with $\rho_n \propto T^4$ and $\tau_{\rm ph} \propto T^{-5}$ for $T \to 0$. However, in the Knudsen limit, Eq. (10) yields $\eta'_n \to \frac{\eta_{\rm ph}}{C\mathcal{K}} \sim du_{\rm ph}\rho_n \to 0$ for $T \to 0$. Accordingly, a peak is obtained at the crossover ($l_{\rm ph} = d$) and the peak of η'_n is shifted upper left as d increases. These behaviors are consistent with the size dependence reported in Ref. [29].

Finally, we evaluated the thermal correction $\delta_{\rm th}$. By substituting $\mathcal{R}_n = \mathcal{R}_s\kappa\rho_n/\eta'_n$ into $F_n/F_s = \frac{c_n}{c_s}\frac{\rho_n}{\rho_s}$ with $c_n = c_D(\mathcal{R}_n)$, we plotted $\delta_{\rm th}$ for $d = 10^{-3}$ m, as in Fig. 4. Although rotons are dominant over phonons and ρ_n/ρ_s is not negligible at temperatures above 0.7 K, the correction was small owing to the cancellation between ρ_n/ρ_s and F_n/F_s as $\delta_{\rm th} \approx (F_n/F_s - \rho_n/\rho_s)/2$. The thermal correction $\delta_{\rm th}$ has a characteristic structure at lower temperatures. For $\mathcal{R}_s \sim 1$ with $\frac{F_n}{F_s} \approx \frac{\mathcal{R}_s\rho_n}{\mathcal{R}_n\rho_s} \approx \frac{\eta'_n}{\rho\kappa}$, $\delta_{\rm th}$ exhibits a structure similar as η'_n by taking the maximum around 0.5 K. The dependence on $\mathcal{R}_s$ is characterized by $\frac{c_n}{c_s} \approx \frac{24c_1}{24c_1+4c_2\sqrt{\mathcal{R}_s}+c_3\mathcal{R}_s}\frac{\eta'_n}{\kappa\rho_n}$; $\delta_{\rm th} \approx \frac{c_n\rho_n}{2c_s\rho_s}$ decreases as $\mathcal{R}_s$ increases. Further, the position of the peak of the contour ($\delta_{\rm th} = 0.1$) shifts from the lower right to upper left with increasing d. This behavior is similar to a shift of the peak of η'_n in Fig. 3 (right).

Summary and prospects. This Letter theoretically proposes a verification of the Reynolds similitude based on the terminal speed measurements of a body falling in superfluid He II. The proposed theory is widely applicable from the Knudsen to hydrodynamic regimes below 1.5 K. If the observables of Eqs. (7) and (8) could reproduce the empirical law (3) with $\mathcal{R} = \mathcal{R}_s$, the Reynolds similitude is considered valid in pure superfluids with quantum kinetic viscosity κ. Spherical objects are preferred as the falling body for a more reliable verification as its drag coefficient is best known in classical hydrodynamics. For example, the drag coefficient for $\mathcal{R}_s \lesssim 10^5$ can be examined for iron balls with a diameter from 10 μm to 5 mm, yielding a terminal speed range of 10^{-4}–2 m/s (Fig. 2) with a small thermal correction below and above 0.2 and 1 K, respectively (Fig. 4). Although the drag coefficients of spheres falling in liquid helium I and II were measured in Refs. [46,47], the concept of quantum viscosity was absent at that time and therefore the drag coefficients should be reexamined by separating the contributions from the superfluid and normal fluid components below 1.5 K. The technique to control uniform rectilinear motions of a superconducting sphere [48] will be useful for testing our hypothesis.

The accuracy of our theory will be improved through future measurements of the drag force or the effective dynamic viscosity η'_n on an object with various shapes in a wide range of temperatures. Furthermore, more experimental data under higher pressures is required to facilitate the precise extension of the theory to the systems of a ^{4}He crystal [14,49–52]. As in the experiments, we can track the detailed motion of falling objects in He II and extract more useful information regarding the terminal speed and the property of the chaotic motion owing to the turbulent wake of the superfluid component. The concept of quantum viscosity facilitates a universal description of the hydrodynamics of superfluids owing to the considerable research data of classical hydrodynamics through the Reynolds similitude. The Reynolds similitude will be useful for investigating turbulent flow in different geometries in quantum liquids He II and ^{3}He-*B* and characterizing superfluid wakes by a moving potential in Bose and Fermi gases of ultracold atoms [9,11,12,53,54].

Acknowledgments. We thank R. Nomura, O. Ishikawa, and H. Yano for useful discussions and information on experiments, and S. Hiramatsu for illustrations. This work was supported by JST, PRESTO Grant No. JPMJPR23O5, Japan, JSPS KAKENHI Grants No. JP18KK0391 and No. JP20H01842, and in part by the Osaka Metropolitan University (OMU) Strategic Research Promotion Project (Priority Research).

[1] O. Reynolds, XXIX. An experimental investigation of the circumstances which determine whether the motion of water shall be direct or sinuous, and of the law of resistance in parallel channels, Philos. Trans. R. Soc. London **174**, 935 (1883).

[2] L. D. Landau and E. M. Lifshitz, *Fluid Mechanics*, Course of Theoretical Physics Vol. 6 (Elsevier, Amsterdam, 2013).

[3] I. M. Khalatnikov, *An Introduction to the Theory of Superfluidity* (CRC Press, Boca Raton, FL, 2018).

[4] C. Nore, M. Abid, and M. E. Brachet, Kolmogorov turbulence in low-temperature superflows, Phys. Rev. Lett. **78**, 3896 (1997).

[5] C. Nore, C. Huepe, and M. E. Brachet, Subcritical dissipation in three-dimensional superflows, Phys. Rev. Lett. **84**, 2191 (2000).

[6] P. A. Davidson, *Turbulence: An Introduction for Scientists and Engineers* (Oxford University Press, Oxford, UK, 2015).

[7] G. E. Volovik, Classical and quantum regimes of superfluid turbulence, J. Exp. Theor. Phys. Lett. **78**, 533 (2003).

[8] J. Maurer and P. Tabeling, Local investigation of superfluid turbulence, Europhys. Lett. **43**, 29 (1998).

[9] M. T. Reeves, T. P. Billam, B. P. Anderson, and A. S. Bradley, Identifying a superfluid Reynolds number via dynamical similarity, Phys. Rev. Lett. **114**, 155302 (2015).

[10] W. Schoepe, Superfluid Reynolds number and the transition from potential flow to turbulence in superfluid ^{4}He at millikelvin temperatures, JETP Lett. **102**, 105 (2015).

[11] W. J. Kwon, J. H. Kim, S. W. Seo, and Y. Shin, Observation of von Kármán vortex street in an atomic superfluid gas, Phys. Rev. Lett. **117**, 245301 (2016).

[12] Y. Lim, Y. Lee, J. Goo, D. Bae, and Y. Shin, Vortex shedding frequency of a moving obstacle in a Bose–Einstein condensate, New J. Phys. **24**, 083020 (2022).

[13] W. Schoepe, Vortex shedding from a microsphere oscillating in superfluid ^{4}He at mK temperatures and from a laser beam moving in a Bose-Einstein condensate, J. Low Temp. Phys. **210**, 539 (2022).

[14] H. Abe, F. Ogasawara, Y. Saitoh, T. Tatara, S. Kimura, R. Nomura, and Y. Okuda, Nucleation of crystals and superfluid droplets in ^{4}He induced by acoustic waves, Phys. Rev. B **71**, 214506 (2005).

[15] J. T. Tough, W. D. McCormick, and J. G. Dash, Viscosity of liquid He II, Phys. Rev. **132**, 2373 (1963).

[16] I. M. Khalatnikov and D. M. Chernikova, Relaxation phenomena in superfluid helium, Sov. Phys. JETP **22**, 1336 (1966).

[17] I. M. Khalatnikov and D. M. Chernikova, Dispersion of first and second sound in superfluid helium, Sov. Phys. JETP **23**, 274 (1966).

[18] K. Nagai, K. Nojima, and A. Hatano, Roton viscosity and roton-roton interactions in superfluid helium, Prog. Theor. Phys. **47**, 355 (1972).

[19] K. Nagai, Roton-roton interactions in superfluid helium. II, Prog. Theor. Phys. **49**, 46 (1973).

[20] D. S. Greywall and G. Ahlers, Second-sound velocity and superfluid density in ^{4}He under pressure near T_λ, Phys. Rev. A **7**, 2145 (1973).

[21] J. Y. T. Worthington and J. U. Trefny, Dependence of helium II viscosity properties on oscillation frequency, J. Low Temp. Phys. **24**, 365 (1976).

[22] J. Maynard, Determination of the thermodynamics of He II from sound-velocity data, Phys. Rev. B **14**, 3868 (1976).

[23] Z. S. Nadirashvili and J. S. Tsakadze, Dependence of helium II viscosity properties on oscillation frequency, J. Low Temp. Phys. **37**, 169 (1979).

[24] M. Lea and P. Fozooni, The roton viscosity of He II under pressure, Phys. Lett. A **93**, 91 (1982).

[25] C.-I. Um, C.-W. Jun, W.-H. Kahng, and T. F. George, Thermal conductivity and viscosity via phonon-phonon, phonon-roton, and roton-roton scattering in thin ^{4}He films, Phys. Rev. B **38**, 8838 (1988).

[26] R. J. Donnelly and C. F. Barenghi, The observed properties of liquid helium at the saturated vapor pressure, J. Phys. Chem. Ref. Data **27**, 1217 (1998).

[27] R. Blaauwgeers, M. Blazkova, M. Človečko, V. Eltsov, R. de Graaf, J. Hosio, M. Krusius, D. Schmoranzer, W. Schoepe, L. Skrbek *et al.*, Quartz tuning fork: Thermometer, pressure- and viscometer for helium liquids, J. Low Temp. Phys. **146**, 537 (2007).

[28] M. Blažková, M. Človečko, E. Gažo, L. Skrbek, and P. Skyba, Quantum turbulence generated and detected by a vibrating quartz fork, J. Low Temp. Phys. **148**, 305 (2007).

[29] A. Zadorozhko, E. Y. Rudavskiĭ, V. Chagovets, G. Sheshin, and Y. A. Kitsenko, Viscosity and relaxation processes in the phonon-roton system of He II, Low Temp. Phys. **35**, 100 (2009).

[30] G. R. Carmichael, Estimation of the drag coefficient of regularly shaped particles in slow flows from morphological descriptors, Ind. Eng. Chem. Process Des. Dev. **21**, 401 (1982).

[31] A. Hölzer and M. Sommerfeld, Lattice Boltzmann simulations to determine drag, lift and torque acting on non-spherical particles, Comput. Fluids **38**, 572 (2009).

[32] S. S. Tiwari, E. Pal, S. Bale, N. Minocha, A. W. Patwardhan, K. Nandakumar, and J. B. Joshi, Flow past a single stationary sphere, 2. Regime mapping and effect of external disturbances, Powder Technol. **365**, 215 (2020).

[33] See Supplemental Material at http://link.aps.org/supplemental/10.1103/PhysRevB.109.L020502 for a detailed discussion on the nonthermal corrections and the concrete formulas of ρ_n, ρ_s, and η_n, which is included Refs. [55,56].

[34] G. W. Stagg, N. G. Parker, and C. F. Barenghi, Superfluid boundary layer, Phys. Rev. Lett. **118**, 135301 (2017).

[35] D. Schmoranzer, M. J. Jackson, V. Tsepelin, M. Poole, A. J. Woods, M. Človečko, and L. Skrbek, Multiple critical velocities in oscillatory flow of superfluid ^{4}He due to quartz tuning forks, Phys. Rev. B **94**, 214503 (2016).

[36] H. A. Nichol, L. Skrbek, P. C. Hendry, and P. V. E. McClintock, Experimental investigation of the macroscopic flow of He II due to an oscillating grid in the zero temperature limit, Phys. Rev. E **70**, 056307 (2004).

[37] J. Jäger, B. Schuderer, and W. Schoepe, Turbulent and laminar drag of superfluid helium on an oscillating microsphere, Phys. Rev. Lett. **74**, 566 (1995).

[38] R. Goto, S. Fujiyama, H. Yano, Y. Nago, N. Hashimoto, K. Obara, O. Ishikawa, M. Tsubota, and T. Hata, Turbulence in boundary flow of superfluid ^{4}He triggered by free vortex rings, Phys. Rev. Lett. **100**, 045301 (2008).

[39] D. Bradley, M. Fear, S. Fisher, A. Guénault, R. Haley, C. Lawson, P. McClintock, G. Pickett, R. Schanen, V. Tsepelin *et al.*, Transition to turbulence for a quartz tuning fork in superfluid ^{4}He, J. Low Temp. Phys. **156**, 116 (2009).

[40] C. S. Barquist, W. G. Jiang, K. Gunther, N. Eng, Y. Lee, and H. B. Chan, Damping of a microelectromechanical oscillator in turbulent superfluid ^{4}He: A probe of quantized vorticity in the ultralow temperature regime, Phys. Rev. B **101**, 174513 (2020).

[41] R. Nomura (private communication).

[42] A. M. Guénault, A. Guthrie, R. P. Haley, S. Kafanov, Y. A. Pashkin, G. R. Pickett, M. Poole, R. Schanen, V. Tsepelin, D. E. Zmeev, E. Collin, O. Maillet, and R. Gazizulin, Probing

superfluid ^{4}He with high-frequency nanomechanical resonators down to millikelvin temperatures, Phys. Rev. B **100**, 020506(R) (2019).

[43] D. Schmoranzer, M. J. Jackson, Š. Midlik, M. Skyba, J. Bahyl, T. Skokánková, V. Tsepelin, and L. Skrbek, Dynamical similarity and instabilities in high-Stokes-number oscillatory flows of superfluid helium, Phys. Rev. B **99**, 054511 (2019).

[44] H. Takeuchi, S. Higashitani, and K. Nagai, Drag force on a high porosity aerogel in liquid ^{3}He, J. Phys.: Conf. Ser. **400**, 012071 (2012).

[45] H. Takeuchi, S. Higashitani, K. Nagai, H. C. Choi, B. H. Moon, N. Masuhara, M. W. Meisel, Y. Lee, and N. Mulders, Knudsen-to-hydrodynamic crossover in liquid ^{3}He in a high-porosity aerogel, Phys. Rev. Lett. **108**, 225307 (2012).

[46] R. A. Laing and H. E. Rorschach, Hydrodynamic drag on spheres moving in liquid helium, Phys. Fluids **4**, 564 (1961).

[47] A. Hemmati, S. Fuzier, E. Bosque, and S. Van Sciver, Drag measurement on an oscillating sphere in helium II, J. Low Temp. Phys. **156**, 71 (2009).

[48] M. Arrayás, F. Bettsworth, R. Haley, R. Schanen, J. L. Trueba, C. Uriarte, V. Zavyalov, and D. Zmeev, Progress on levitating a sphere in cryogenic fluids, J. Low Temp. Phys. **212**, 363 (2023).

[49] R. Nomura, T. Yoshida, A. Tachiki, and Y. Okuda, Falling ^{4}He crystals in superfluid, New J. Phys. **16**, 113022 (2014).

[50] V. L. Tsymbalenko, Dynamics of a ^{4}He quantum crystal in the superfluid liquid, J. Low Temp. Phys. **201**, 526 (2020).

[51] R. Nomura and Y. Okuda, Colloquium: Quantum crystallizations of ^{4}He in superfluid far from equilibrium, Rev. Mod. Phys. **92**, 041003 (2020).

[52] V. Tsymbalenko, Effect of the phase boundary kinetics of a helium crystal on motion in a superfluid liquid, J. Low Temp. Phys. **208**, 316 (2022).

[53] K. Sasaki, N. Suzuki, and H. Saito, Bénard–von Kármán vortex street in a Bose-Einstein condensate, Phys. Rev. Lett. **104**, 150404 (2010).

[54] J. W. Park, B. Ko, and Y. Shin, Critical vortex shedding in a strongly interacting fermionic superfluid, Phys. Rev. Lett. **121**, 225301 (2018).

[55] R. J. Donnelly, *Quantized Vortices in Helium II* (Cambridge University Press, Cambridge, UK, 1991), Vol. 2.

[56] H. Takeuchi, K. Kasamatsu, and M. Tsubota, Spontaneous radiation and amplification of Kelvin waves on quantized vortices in Bose-Einstein condensates, Phys. Rev. A **79**, 033619 (2009).